



**Manchester
Metropolitan
University**

Wang, Tiancheng, Randviir, Edward P ORCID logoORCID:
<https://orcid.org/0000-0001-7252-8494> and Banks, Craig E ORCID logoOR-
CID: <https://orcid.org/0000-0002-0756-9764> (2014) Detection of theophylline
utilising portable electrochemical sensors. Analyst, 139 (8). pp. 2000-2003.
ISSN 0003-2654

Downloaded from: <https://e-space.mmu.ac.uk/596033/>

Version: Published Version

Publisher: Royal Society of Chemistry

DOI: <https://doi.org/10.1039/c4an00065j>

Usage rights: Creative Commons: Attribution 3.0

Please cite the published version

<https://e-space.mmu.ac.uk>

Detection of theophylline utilising portable electrochemical sensors

Cite this: *Analyst*, 2014, **139**, 2000

Tiancheng Wang, Edward P. Randviir and Craig E. Banks*

Received 10th January 2014
Accepted 25th January 2014

DOI: 10.1039/c4an00065j

www.rsc.org/analyst

The electrochemical oxidation of theophylline (TP) is investigated utilising screen-printed electrodes. Through thorough investigation of pH, we propose a reaction mechanism, finding that the oxidation of TP is stable over a wide pH range, in particular under acidic conditions. Conversely under alkaline conditions, theophylline fouls the electrode surface. The screen-printed carbon sensors are applied towards the electroanalytical sensing of TP with a remarkable amount of success in aqueous solution at physiological pH. The screen-printed sensors have been shown to be applicable to the detection of TP at unharmed, medically relevant (55–110 μM), and toxic concentrations in aqueous media at physiological pH. Thus this work presents a proof-of-concept approach towards TP detection utilising sensors commonly implemented in point-of-care applications.

Introduction

Theophylline (TP) is a commonly utilised drug clinically for treatment of respiratory diseases such as asthma due to its bronchodilatory effects.¹ However TP exhibits a narrow safety range² which means technologies are required which have the ability to monitor the levels of TP within the body. Currently the clinical practise requires the clinic to regularly monitor plasma by taking blood samples from patients, less chronic conditions may develop.³ Such blood samples are fairly large (in excess of 25 mL and normally more than one sample is taken at once) and thus patients may consider providing these regular blood samples as problematic. Nevertheless theophylline still has to be monitored due to its toxicological effects; thus scaling down the detection technology for use on-site, with small sample sizes (<100 μL), is an area worthy of serious consideration.

Current laboratory procedures for theophylline detection include radioimmunoassay,⁴ high performance liquid chromatography,⁵ and fluorescence polarization immunoassay.⁶ However such methods require skilled personnel, sample pre-treatment, and long analysis times. Consequently electrochemists have taken the opportunity to study the electrochemical oxidation of theophylline utilising a variety of electrode substrates.^{7–11} These praiseworthy efforts of researchers have rarely been mimicked with screen-printed electrodes (SPEs), however, these screen-printed sensors which have been reported require the design of complicated electrode composites.^{12,13} Such composites contain either enzymes or

recognition proteins which make the electrochemistry complex. Surprisingly however, the direct oxidation of theophylline utilising SPEs appears to be overlooked in the literature. Hence, for the purpose of completeness we provide the electrochemical activities of three screen-printed sensors (edge-plane-like, basal-plane-like, and single-walled carbon nanotube SPEs) and compare to standard laboratory electrodes including gold, highly ordered pyrolytic graphite, glassy carbon, and boron-doped diamond.

Experimental

All chemicals were of the highest grade available, used without further purification, and obtained from Sigma Aldrich (UK). All aqueous solutions were made using deionised water of resistivity no less than 18.2 M Ω cm. Several buffer solutions were appropriately selected: 0.1 M acetate buffer (pH 4.0); 0.1 M Phosphate Buffer Solution (PBS) (pH 7.4); and 0.1 M borate buffer (pH 11.5). For pH 1.0, 0.1 M sulphuric acid was utilised as the solvent. Theophylline stock solutions were prepared in each appropriate pH prior to testing. Voltammetric data were obtained utilising an Ivium CompactStat™ (Netherlands) potentiostat. SPEs (edge plane-like, termed ESPE and basal plane-like, termed BSPE) were fabricated in-house as described previously.¹⁴ Briefly, a relevant carbon ink formulation for efficient connection of the three electrodes was printed onto a flexible polyester film and cured in an oven at 60 °C for 30 minutes. Next a silver/silver chloride reference electrode was included by screen-printing Ag/AgCl paste and subsequently curing at 60 °C for 30 minutes. Finally, a dielectric paste was printed on top to define the electrodes (3 mm working electrode) and protect the connections. Further information regarding the inks can be found in ref. 15. The single-walled

Faculty of Science and Engineering, School of Chemistry and the Environment, Division of Chemistry and Environmental Science, Manchester Metropolitan University, Chester Street, Manchester M1 5GD, Lancs, UK. E-mail: c.banks@mmu.ac.uk; Web: <http://www.craigbanksresearch.com>; Fax: +44 (0)1612476831; Tel: +44 (0)1612471196



carbon nanotube SPEs were made (termed SW-SPE) as above, except that commercially available single-walled carbon nanotube ink was printed over the working electrode only following the third curing procedure.¹⁶ Conventional electrodes (3 mm Glassy Carbon (GC), 4.9 mm Edge Plane and Basal Plane Pyrolytic Graphite (EPPG/BPPG), 3 mm gold, 3 mm Boron Doped Diamond (BDD)) were obtained commercially from Le Carbone Ltd., Sussex, U.K. and were polished to a mirror-like shine utilising diamond spray of decreasing particle size. A saturated calomel electrode (SCE) was utilised as a reference and a platinum wire as an auxiliary electrode, unless otherwise stated.

Results and discussion

Electrode investigation

Attention is first turned towards the electrochemical response of 1 mM theophylline at several electrode substrates at physiological pH. Fig. 1 compares all electrode substrates investigated. Inspection of Fig. 1 reveals a general trend where the peak potential decreases as the peak current density increases; this is particularly evident for the case of electrodes such as EPPG which exhibits a peak potential of +1.00 V and an average peak current of $191 \mu\text{A cm}^{-2}$ (% RSD = 5%; $N = 3$). Conversely, by taking the gold electrode as an example, a large overpotential (+1.17 V) is required to drive the electrochemical oxidation of TP which compromises on both the average observed current density of $57 \mu\text{A cm}^{-2}$ and the reproducibility (% RSD = 46%; $N = 3$). Turning attention to the screen-printed electrodes, we investigate a trio of SPEs which are electrochemically divergent. Fig. 1 shows the edge plane-like SPE (ESPE) and the single-walled carbon nanotube SPE (SW-SPE) exhibiting similar behaviour, with peak potentials corresponding to +1.04 V and +1.03 V, respectively.

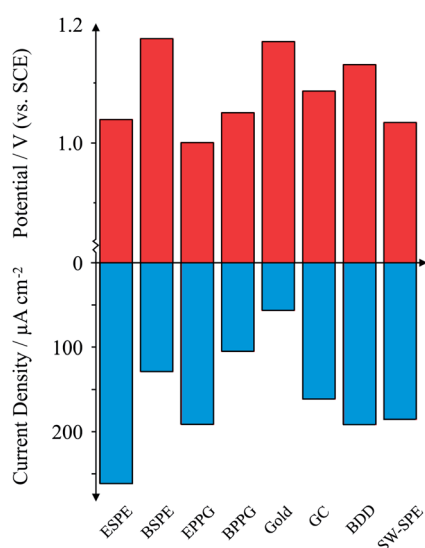


Fig. 1 Graphical representation of peak current densities (blue) and peak potentials (red) for the series of electrodes utilised within this work. All experiments were conducted using 1 mM TP in 0.1 M PBS (pH 7.4). Scan rate: 100 mV s^{-1} .

Similar reactivities are likely due to the edge-plane content of the respective electrodes. Remarkably, the ESPE exhibits the highest peak current density of all electrodes studied here, corresponding to an average value of $262 \mu\text{A cm}^{-2}$ and furthermore exhibiting a % RSD of 5% ($N = 3$); such an electrode could prove to be useful for electroanalytical sensing of TP. Conversely, the basal plane-like SPE (BSPE) exhibits a high peak potential (+1.17 V) and a low peak current density of $129 \mu\text{A cm}^{-2}$, similar to the case of the gold and basal plane pyrolytic graphite (BPPG) electrodes. Though the observed current densities are not as high for BSPE and SW-SPE as that observed for EPPG, they still exhibit a magnitude and reproducibility (<5%) which are useful for electroanalytical sensing. Glassy Carbon (GC) and Boron Doped Diamond (BDD) both exhibit high peak potentials and low currents. We continue to investigate the edge-plane-like SPE in terms of pH and electroanalytical capabilities; the SW-SPE could potentially be also used but we see no further benefits of the carbon nanotubes in this instance, generally due to cost implications.

pH

To optimise the electroanalytical conditions it is necessary to investigate the effect of pH on the observed peak potentials and currents for TP. Fig. 2 depicts voltammetric profiles of 1 mM TP, corresponding to changes in pH. One can immediately observe that the peak potentials increase as the pH decreases (inset), yet the relative magnitude of the peak current fluctuates, indicating that the efficiency of electron transfer for TP is pH dependent. The plot of peak potential *versus* pH, presented in the inset of Fig. 2, illustrates the pH dependence of peak potential for this system which is linear from pH 1 to 8.5, beyond which there is deviation; this is in agreement with its pK_a , reported to be ~ 8.6 .¹⁷ The slope of the graph inset in Fig. 2 corresponds to 61.7 mV pH^{-1} ($R^2 = 0.994$), corresponding to approximately an equal number of protons and electrons transferred. Above pH 8.5, a secondary wave appears (not reported), masking the analytical peak. We believe further peaks to be a result of electrode fouling, which was apparent under strongly alkaline conditions. Given the lack in change of mechanism over the large pH range prior to the pK_a , we consequently select physiological pH for electroanalysis which is presented later.

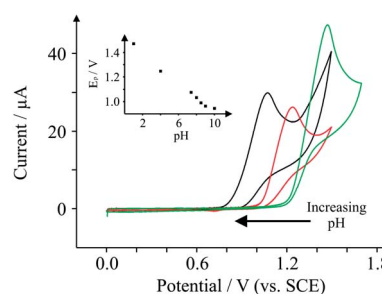
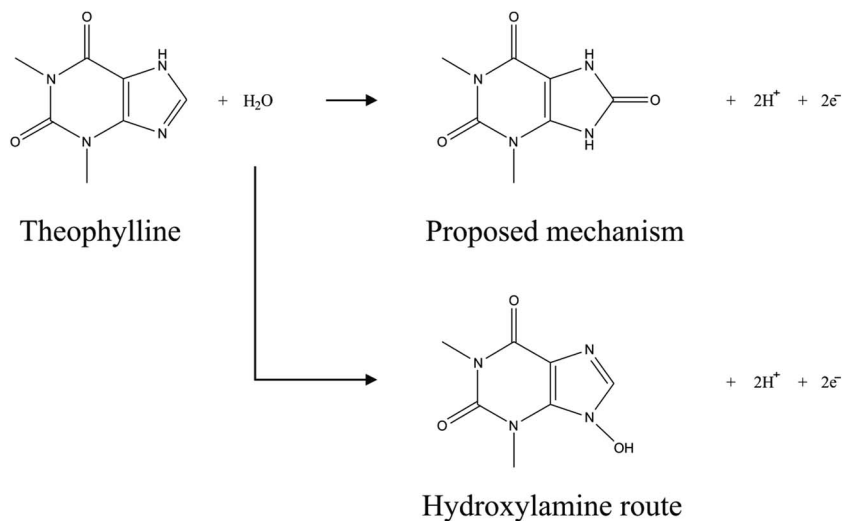


Fig. 2 Cyclic voltammetric profiles obtained for 1 mM TP using an ESPE working electrode under various conditions: pH 1.0 (green); pH 4.2 (red); and pH 7.4 (black). Scan rate: 100 mV s^{-1} . Inset: peak potential *versus* pH for the entire pH range utilised.





Scheme 1 Structure of TP and two possible reaction mechanisms.

The mechanism of TP oxidation is next considered by taking into account the pH. The structure of TP is given in Scheme 1, alongside two proposed reaction mechanisms. Given that TP has a structure which can be thought of as analogous to guanine, the proposed mechanism involves a two electron two proton oxidation of the aromatic carbon sandwiched between two electron-withdrawing nitrogen heteroatoms, as is in the case of the structurally similar guanine.¹⁸ Of course, under highly basic conditions the oxidation of the nitrogen heteroatom to a hydroxylamine is possible in small quantities, yet we believe that the formation of the carbonyl is more likely. The fact that the mechanism does not change dramatically above the pK_a acts as support for this mechanism.

Electroanalytical detection of theophylline

To demonstrate the applicability of SPEs to TP, we investigate the effect of peak currents with respect to the concentration of TP present within a buffer solution at physiological pH. Fig. 3 depicts the effect of peak current as the concentration of TP in pH 7.4 PBS increases. The electroanalytical peak observed at *ca.* +1.0 V increases linearly as a function of TP concentration, as depicted in the inset of Fig. 3: $I_p/\mu A = 12.28 \mu A \text{ mM}^{-1} + 0.91 \mu A$;

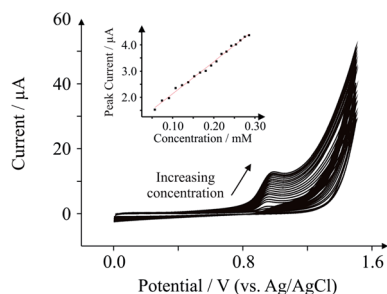


Fig. 3 Electroanalytical cyclic voltammetric profiles of TP utilising an ESPE working electrode. The on-board carbon auxiliary and Ag/AgCl reference electrode is utilised in this instance. Scan rate: 100 mV s^{-1} .

$N = 18$; $R^2 = 0.994$, with a limit of detection of $10 \mu\text{M}$. The concentrations studied here range from $50\text{--}290 \mu\text{M}$, which falls within the safe concentrations found in the plasma of medicinal TP users ($55\text{--}110 \mu\text{M}$ – anything higher is considered dangerous),¹⁹ indicating that our protocol is potentially acceptable for TP detection in plasma for clinical screening applications. Furthermore the sensors exhibit % RSD values of no more than 5% ($N = 3$) which is within the constraints of acceptable (electro)analytical chemistry.

Conclusions

The detection of TP utilising SPEs has been described. Screen-printed sensors such as SW-SPE and BSPE replicate standard macroelectrodes such as EPPG with a relatively small loss of peak current density and increase in peak potential. Compared to other working electrodes such as gold, BPPG and GC, all the SPEs are superior in terms of peak current density and peak potential. ESPE however outperforms EPPG in terms of peak current density and thus is more suitable than EPPG for electroanalytical sensing of TP. SPEs also carry the added benefit of application to point-of-care systems. The SPEs are shown to be applicable to the detection of TP at both acidic and physiological pH, yet display unstable voltammetric waves under highly alkaline conditions. A two proton two electron mechanism is proposed for the electrochemical oxidation of TP as a result of the pH investigations. The electrodes also display a remarkably high level of electroanalytical linearity at physiological pH. In the future, such electrodes need to be investigated further towards medicinal formulations containing TP, as well as plasma samples for screening purposes. Additionally, exploring the possibility of screen-printed microbands and arrays could prove to be important as the improved current densities produced by such sensing platforms could prove to be beneficial for electroanalytical applications. Such work, in addition to previous work regarding SPEs, highlights the range of opportunities for such technologies and as a result we believe the possibilities for SPE application are essentially



limitless in terms of electrochemically screening molecules for point-of-care applications.

References

- 1 P. J. Barnes and R. A. Pauwels, *Eur. Respir. J.*, 1994, **7**, 579–591.
- 2 A. H. Dawson and I. M. Whyte, *Br. J. Clin. Pharmacol.*, 1999, **48**, 278–283.
- 3 M. Shannon, *Ann. Intern. Med.*, 1993, **119**, 1161–1167.
- 4 C. E. Cook, M. E. Twine, M. Myers, E. Amerson, J. A. Kepler and G. F. Taylor, *Res. Commun. Chem. Pathol. Pharmacol.*, 1976, **13**, 497–505.
- 5 B. Srdjenovic, V. Djordjevic-Milic, N. Grujic, R. Injac and Z. Lepojevic, *J. Chromatogr. Sci.*, 2008, **46**, 144–149.
- 6 M. E. Jolley, *J. Anal. Toxicol.*, 1981, **5**, 236–240.
- 7 E. E. Ferapontova, E. M. Olsen and K. V. Gothelf, *J. Am. Chem. Soc.*, 2008, **130**, 4256–4258.
- 8 Y.-H. Zhu, Z.-L. Zhang and D.-W. Pang, *J. Electroanal. Chem.*, 2005, **581**, 303–309.
- 9 N. Spătaru, B. V. Sarada, D. A. Tryk and A. Fujishima, *Electroanalysis*, 2002, **14**, 721–728.
- 10 Y. V. Ulyanova, A. E. Blackwell and S. D. Minter, *Analyst*, 2006, **131**, 257–261.
- 11 B. H. Hansen and G. Dryhurst, *J. Electroanal. Chem. Interfacial Electrochem.*, 1971, **32**, 405–414.
- 12 N. C. Foulds, J. M. Wilshire and M. J. Green, *Anal. Chim. Acta*, 1990, **229**, 57–62.
- 13 K. S. Lee, T.-H. Kim, M.-C. Shin, W.-Y. Lee and J.-K. Park, *Anal. Chim. Acta*, 1999, **380**, 17–26.
- 14 N. A. Choudry, D. K. Kampouris, R. O. Kadara and C. E. Banks, *Electrochem. Commun.*, 2010, **12**, 6–9.
- 15 E. P. Randviir, D. A. C. Brownson, J. P. Metters, R. O. Kadara and C. E. Banks, *Phys. Chem. Chem. Phys.*, 2014, **16**, 4598–4611.
- 16 E. P. Randviir, J. P. Metters, J. Stainton and C. E. Banks, *Analyst*, 2013, **138**, 2970–2981.
- 17 A. V. Trask, W. D. S. Motherwell and W. Jones, *Int. J. Pharm.*, 2006, **320**, 114–123.
- 18 R. N. Goyal, B. K. Puri and N. Jain, *J. Chem. Soc., Perkin Trans. 2*, 2001, 832–837.
- 19 P. A. Mitenko and R. I. Ogilvie, *N. Engl. J. Med.*, 1973, **289**, 600–603.

